



Mmf1p Couples Amino Acid Metabolism to Mitochondrial DNA Maintenance in *Saccharomyces cerevisiae*

Dustin C. Ernst,^{a*} Diana M. Downs^a

^aDepartment of Microbiology, University of Georgia, Athens, Georgia, USA

ABSTRACT A variety of metabolic deficiencies and human diseases arise from the disruption of mitochondrial enzymes and/or loss of mitochondrial DNA. Mounting evidence shows that eukaryotes have conserved enzymes that prevent the accumulation of reactive metabolites that cause stress inside the mitochondrion. 2-Aminoacrylate is a reactive enamine generated by pyridoxal 5'-phosphate-dependent α,β -eliminases as an obligatory intermediate in the breakdown of serine. In prokaryotes, members of the broadly conserved RidA family (PF14588) prevent metabolic stress by deaminating 2-aminoacrylate to pyruvate. Here, we demonstrate that unmanaged 2-aminoacrylate accumulation in *Saccharomyces cerevisiae* mitochondria causes transient metabolic stress and the irreversible loss of mitochondrial DNA. The RidA family protein Mmf1p deaminates 2-aminoacrylate, preempting metabolic stress and loss of the mitochondrial genome. Disruption of the mitochondrial pyridoxal 5'-phosphate-dependent serine dehydratases (Ilv1p and Cha1p) prevents 2-aminoacrylate formation, avoiding stress in the absence of Mmf1p. Furthermore, chelation of iron in the growth medium improves maintenance of the mitochondrial genome in yeast challenged with 2-aminoacrylate, suggesting that 2-aminoacrylate-dependent loss of mitochondrial DNA is influenced by disruption of iron homeostasis. Taken together, the data indicate that Mmf1p indirectly contributes to mitochondrial DNA maintenance by preventing 2-aminoacrylate stress derived from mitochondrial amino acid metabolism.

IMPORTANCE Deleterious reactive metabolites are produced as a consequence of many intracellular biochemical transformations. Importantly, reactive metabolites that appear short-lived *in vitro* have the potential to persist within intracellular environments, leading to pervasive cell damage and diminished fitness. To overcome metabolite damage, organisms utilize enzymatic reactive-metabolite defense systems to rid the cell of deleterious metabolites. In this report, we describe the importance of the RidA/YER057c/UK114 enamine/imine deaminase family in preventing 2-aminoacrylate stress in yeast. *Saccharomyces cerevisiae* lacking the enamine/imine deaminase Mmf1p was shown to experience pleiotropic growth defects and fails to maintain its mitochondrial genome. Our results provide the first line of evidence that uncontrolled 2-aminoacrylate stress derived from mitochondrial serine metabolism can negatively impact mitochondrial DNA maintenance in eukaryotes.

KEYWORDS 2-aminoacrylate, RidA, enamine deaminase, metabolite stress, mitochondrial genome

RidA/YER057c/UK114 (Rid) family proteins (PF14588) are ubiquitous; phylogenetic analysis identified the archetypal RidA throughout all three domains of life, with additional subgroups (Rid1 to Rid7) present in prokaryotes (1, 2). Biochemical genetic studies in the bacterium *Salmonella enterica* determined that RidA proteins are deaminases that hydrolyze the reactive enamine 2-aminoacrylate (2AA), and other enamine/

Received 12 January 2018 Accepted 18 January 2018 Published 27 February 2018

Citation Ernst DC, Downs DM. 2018. Mmf1p couples amino acid metabolism to mitochondrial DNA maintenance in *Saccharomyces cerevisiae*. mBio 9:e00084-18. <https://doi.org/10.1128/mBio.00084-18>.

Editor Susan Gottesman, National Cancer Institute

Copyright © 2018 Ernst and Downs. This is an open-access article distributed under the terms of the [Creative Commons Attribution 4.0 International license](https://creativecommons.org/licenses/by/4.0/).

Address correspondence to Diana M. Downs, dmdowns@uga.edu.

* Present address: Dustin C. Ernst, University of California, San Diego, La Jolla, CA, USA.

This article is a direct contribution from a Fellow of the American Academy of Microbiology. Solicited external reviewers: James Imlay, University of Illinois at Urbana Champaign; Josep Casadesus, Universidad de Sevilla; Mark Johnston, University of Colorado School of Medicine.

imine substrates, to ketoacids (3–8). In cellular metabolism, 2AA is generated by pyridoxal 5'-phosphate (PLP)-dependent α,β -eliminase enzymes as an intermediate in the conversion of amino acids to pyruvate (3, 4, 7). Following release from the enzyme, 2AA can be spontaneously converted to pyruvate by solvent water (7). Although 2AA can covalently modify enzymes *in vitro* (9–15), the potential for intracellular enamine damage was initially dismissed because of the short (~1.5-s) half-life of 2AA in water (16). However, biochemical and genetic data demonstrate that in the absence of RidA, unbound 2AA persists *in vivo* and inactivates PLP-dependent enzymes (1, 17, 18). These data indicate that the cellular milieu lacks sufficient free water to rapidly hydrolyze 2AA and provides the framework for phenotypes displayed by *ridA* mutants (6, 17–20). The prevalence of PLP-dependent enzymes (including α,β -eliminases) involved in basic metabolic pathways, coupled with the broad distribution of RidA homologues, suggests that 2AA stress likely occurs in diverse organisms.

Little is known about eukaryotic Rid proteins, although early reports suggested involvement in a variety of cellular processes mediated by undefined mechanisms (21–30). Interestingly, the mitochondrial RidA protein Mmf1p (mitochondrial matrix factor) influences mitochondrial DNA (mtDNA) stability in *Saccharomyces cerevisiae* (29, 30). Unlike some mitochondrial DNA maintenance factors (e.g., Abf2p) (31), Mmf1p does not bind and stabilize the mitochondrial nucleoid directly (29). Characterization of enamine deaminase activity *in vitro* and genetic complementation analyses *in vivo* suggest that RidA proteins from the three domains of life share a conserved cellular function (7, 28). The biochemical activity of RidA from yeast (e.g., Mmf1p) was not addressed by those previous studies. Here, we demonstrate that 2AA generation provokes the irreversible loss of mtDNA in *S. cerevisiae* lacking Mmf1p. The data indicate that iron present in the growth medium influences the stability of mtDNA when 2AA stress is encountered. Furthermore, 2AA stress elicits a growth defect that is distinct from the respiratory deficiency caused by mtDNA loss. This report establishes the role of Mmf1p in indirectly stabilizing mtDNA by preventing 2AA stress in a eukaryote and highlights damage that results from reactive metabolite imbalance in mitochondria.

RESULTS

Disruption of *MMF1* leads to a growth defect and loss of mtDNA. The *MMF1* locus of the haploid *S. cerevisiae* strain YJF153 (32) was replaced with a drug cassette by targeted gene disruption, and the drug marker was resolved to generate mutant strain DMy22 (*mmf1* Δ 0). A plasmid expressing *MMF1* or an empty vector (pSF-TEF1-G418; Sigma) was introduced into DMy22, the wild-type parent (ρ^+), and a chemically induced cytoplasmic petite (ρ^-) strain derived from the wild-type strain. The resulting strains were assessed for growth on minimal medium containing a fermentable (dextrose [D]) or nonfermentable (glycerol [G]) carbon substrate (Fig. 1A). The *mmf1* Δ mutant had two significant growth phenotypes: (i) an inability to grow on glycerol and (ii) a reduced ability to grow on dextrose. Plasmid-borne *MMF1* failed to restore growth on glycerol, consistent with the irreversible loss or mutation of mtDNA observed in ρ^0 or ρ^- cytoplasmic petites (33) (Fig. 1A). Results of deconvolution microscopy confirmed that the *mmf1* Δ mutant lacked detectable mtDNA and therefore was likely a ρ^0 -cytoplasmic petite (see below). In contrast, growth of the *mmf1* Δ mutant on dextrose was restored to a level similar to that of the ρ^- control by providing plasmid-borne *MMF1*. This indicated that transient metabolic deficiencies distinguishable from the respiratory defect were encountered by strains lacking Mmf1p. The addition of isoleucine and, to a lesser extent, threonine (an isoleucine precursor) restored growth of the ρ^0 *mmf1* Δ mutant on dextrose (Fig. 1B) but not on glycerol. Together, these data distinguished the reversible and irreversible consequences of the *mmf1* Δ mutation, and each was considered in turn.

Ilv1p-generated 2-aminoacrylate causes a growth defect in the absence of Mmf1p. The data support a model where both the growth defect and mtDNA loss are consequences of the toxic accumulation of 2AA in mitochondria lacking Mmf1p. The

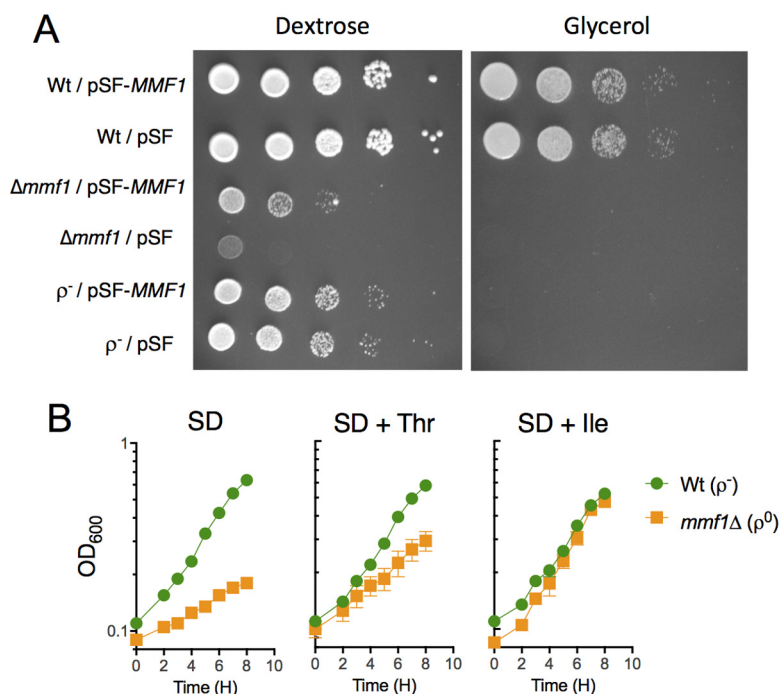


FIG 1 Yeast lacking Mmf1p cannot respire glycerol and have a growth defect on dextrose. (A) Growth of wild-type (ρ^+), petite wild-type (ρ^-), and $mmf1\Delta$ mutant strains on synthetic dextrose (SD) and synthetic glycerol (SG) solid media. An *MMF1* expression plasmid (pSF-*MMF1*) or the empty vector (pSF) was transformed into each strain prior to growth analyses. The numbers of cells from each strain were the same across the dilutions. (B) Growth of a ρ^0 $mmf1\Delta$ mutant and petite wild-type (ρ^-) strain in liquid SD medium supplemented with isoleucine or threonine as indicated. Data indicate averages and standard deviations of results from three independent cultures.

growth defect of a ρ^0 $mmf1\Delta$ mutant on dextrose is reminiscent of a *ridA* mutant phenotype in *S. enterica* (19). In this case, 2AA generated by serine/threonine dehydratase (IlvA; EC 4.3.1.19) accumulates and compromises growth. Isoleucine allosterically inhibits IlvA, prevents 2AA generation, and restores growth in defined medium. Two nuclear encoded serine/threonine dehydratases (EC 4.3.1.19) are active in the *S. cerevisiae* mitochondrion. Ilv1p is the biosynthetic serine/threonine dehydratase required for isoleucine biosynthesis (34), and Cha1p is a catabolic dehydratase induced by serine or threonine (35). Much like the bacterial enzyme IlvA, Ilv1p catalyzes the first committed step in isoleucine biosynthesis, is subject to feedback inhibition by isoleucine, and uses serine as a substrate as an alternative to threonine (36) (Fig. 2A). *In vitro*, Ilv1p dehydrated serine and released 2AA, which Mmf1p used as a substrate, leading to an increased rate of pyruvate formation (Fig. 2B). On a per-mole basis, the 2AA-hydrolyzing activity of Mmf1p was indistinguishable from that of the well-characterized RidA enzyme from *S. enterica* (Fig. 2B). These data support the hypothesis that the absence of Mmf1p leads to accumulation of 2AA following serine dehydration.

Taken together, the data favored the scenario depicted in Fig. 2A and suggested that the growth-stimulating role of isoleucine was exerted via the allosteric inhibition of Ilv1p. If true, preventing allosteric inhibition of Ilv1p would abolish the benefit of the presence of isoleucine in cells lacking Mmf1p. To test this hypothesis, an allosterically resistant variant of Ilv1p (Ilv1p^{R416F}) was generated using an allosterically resistant variant of *Escherichia coli* IlvA (IlvA^{R362F}) as a template (37). *In vitro*, recombinant Ilv1p_(46–576)^{R416F} was insensitive to isoleucine concentrations that completely inhibited the wild-type enzyme (Fig. 2C). Importantly, the catalytic efficiency of serine dehydration by the variant enzyme was not significantly different from the efficiency seen with the wild-type enzyme (Fig. 2D). Wild-type *ILV1* was replaced with the full-length allele (*ILV1-1*) encoding Ilv1p^{R416F} to generate a strain where 2AA production by Ilv1p could

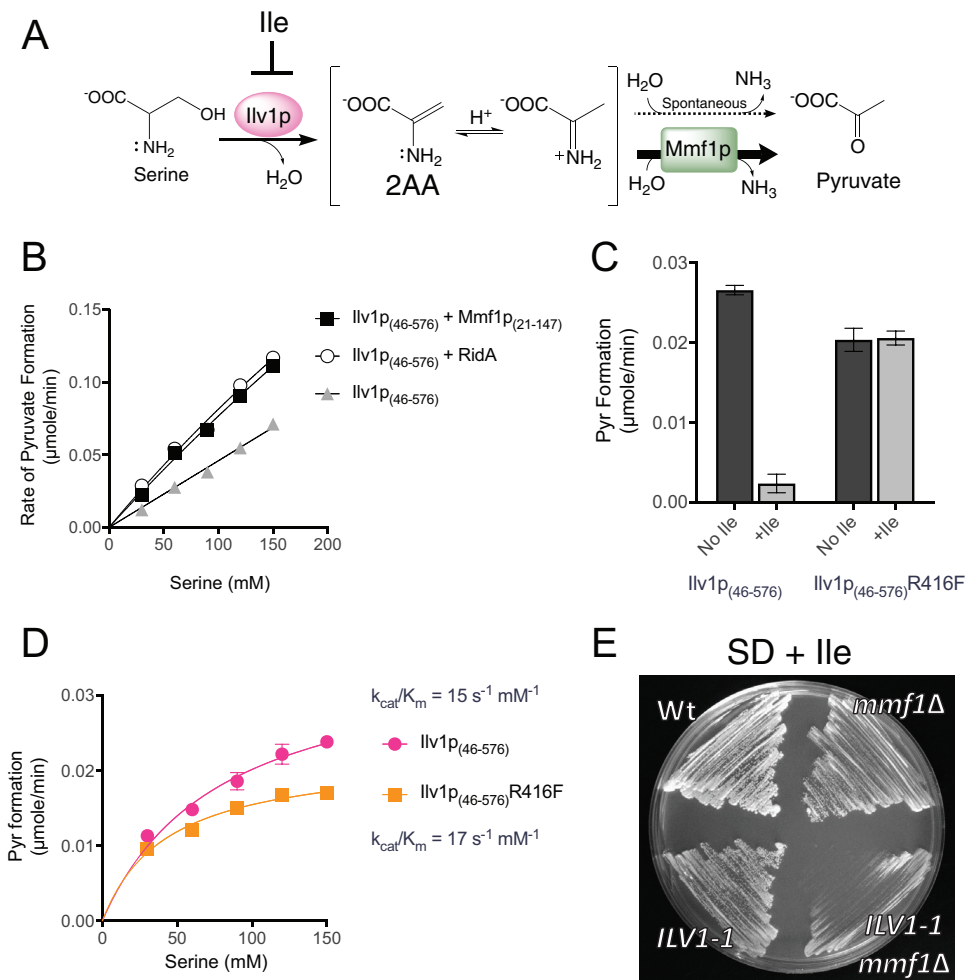


FIG 2 Ilv1p generates 2AA stress in yeast lacking Mmf1p. (A) Scheme of Ilv1p-mediated pyruvate formation, showing 2AA as an unbound intermediate that can be hydrolyzed to pyruvate by solvent water or Mmf1p. Isoleucine allosterically inhibits Ilv1p activity and prevents 2AA formation. Cha1p catalyzes the same reaction as Ilv1p but is not allosterically regulated. (B) The rates of conversion of serine to pyruvate by Ilv1p₍₄₆₋₅₇₆₎ were enhanced similarly by adding Mmf1p₍₂₁₋₁₄₇₎ (*S. cerevisiae*) or RidA (*S. enterica*). Data represent averages and standard deviations of results from three independent experiments, with error bars not exceeding the symbol boundaries. (C) The serine dehydratase activity of the purified Ilv1p₍₄₆₋₅₇₆₎-R416F variant was insensitive to a concentration of isoleucine (3.3 mM) that completely inhibited the wild-type enzyme. Data represent averages and standard deviations of results from three independent experiments. (D) Ilv1p₍₄₆₋₅₇₆₎-R416F has levels of catalytic efficiency for serine dehydration similar to those seen with the wild-type enzyme. Data indicate averages and standard deviations of results from three independent experiments. (E) Inserting the *ILV1-1* allele encoding Ilv1p^{R416F} into a ρ^0 *mmf1* Δ strain prevented isoleucine from restoring full growth to the double mutant compared to the ρ^0 *mmf1* Δ single mutant following 48 h of incubation on solid medium consisting of SD plus Ile (SD + Ile) (1 mM) at 30°C. Wt, wild type.

not be inhibited. Isoleucine failed to completely reverse the growth defect of the *mmf1* Δ mutant strain expressing Ilv1p^{R416F} in minimal synthetic dextrose (SD) medium (Fig. 2E). Therefore, isoleucine improves growth of the *mmf1* Δ mutant strain in part through allosteric inhibition of Ilv1p and not by satisfying an isoleucine requirement. Taken together, these data show that Ilv1p generates 2AA from endogenous serine and that growth is limited unless Mmf1p or isoleucine quenches 2AA or inhibits Ilv1p activity, respectively.

Cha1p increases 2-aminoacrylate stress when exogenous serine is present. The ρ^0 *mmf1* Δ mutant characterized as described above was constructed on rich (yeast extract-peptone-dextrose [YPD]) medium containing isoleucine, so feedback inhibition prevented Ilv1p from generating significant 2AA. Therefore, if 2AA stress were to contribute to mtDNA loss, an additional enzyme would be required to generate 2AA in

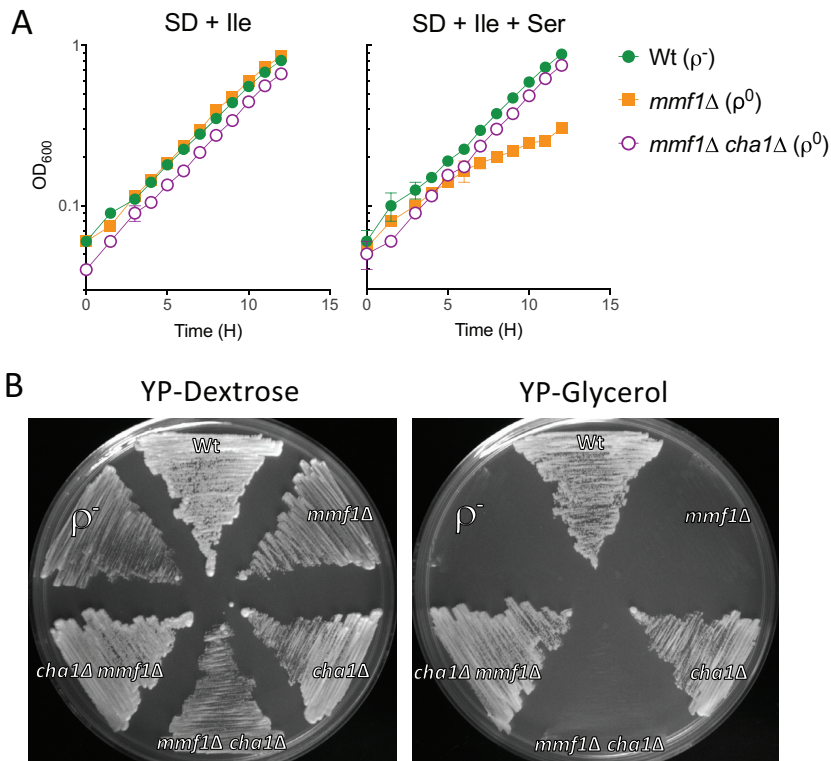


FIG 3 Cha1p contributes to 2AA generation when serine is provided exogenously. (A) Disruption of *CHA1* prevents conversion of exogenous serine (5 mM) to 2AA, thereby alleviating exogenous serine sensitivity in a ρ^0 *mmf1* Δ *cha1* Δ background. Data are displayed as averages and standard deviations of results from three independent experiments. (B) Preventing 2AA production by simultaneously inhibiting the activity of *llv1p* (with isoleucine) and deleting *CHA1* renders *Mmf1p* nonessential for mtDNA maintenance despite the presence of serine in the growth medium. All mutants were constructed in the order indicated by the genotype and selected on YPD medium prior to streaking on the displayed YPD or YPG plates. The *mmf1* Δ *cha1* Δ strain (DMY17) was constructed independently from the *cha1* Δ *mmf1* Δ strain (DMY20), and the order in which the mutations were introduced differed as indicated in the text. Growth was recorded after 48 h at 30°C.

the presence of isoleucine. The catabolic Ser/Thr dehydratase Cha1p is a logical source of 2AA, since *CHA1* expression is induced by serine, which is present in YPD, and since the enzyme is insensitive to regulation by isoleucine (35). Growth analysis in SD medium plus isoleucine, with or without serine, confirmed that Cha1p contributed to 2AA stress in the absence of *Mmf1p* (Fig. 3A). Both the ρ^0 *mmf1* Δ and ρ^0 *mmf1* Δ *cha1* Δ mutants grew in medium with isoleucine, but the addition of serine compromised growth only of the ρ^0 *mmf1* Δ mutant, indicating *CHA1* is required for sensitivity to exogenous serine. These data indicate that 2AA is produced following induction of Cha1p by exogenous serine and that *llv1p* is inhibited by isoleucine via feedback inhibition. The increased level of 2AA compromised growth in the absence of *MMF1*. Unlike the results seen with a *ridA* mutant in *S. enterica* (38), the growth defect of the ρ^0 *mmf1* Δ mutant was not reversed by the addition of common nutritional supplements (i.e., amino acids or vitamins). This result suggests that the cellular deficiencies underpinning the 2AA-dependent growth defect of *mmf1* Δ mutant strains in minimal medium are more complex than those caused by a single compromised enzyme.

Disruption of serine dehydratase-dependent 2-aminoacrylate production preserves mtDNA in the absence of *MMF1*. Despite the connection between *Mmf1p* and 2AA, it remained possible that the irreversible loss of mtDNA in an *mmf1* Δ mutant strain was unrelated to 2AA accumulation. However, data from order-dependent genetic manipulations and growth analyses demonstrate that 2AA stress specifically caused mtDNA loss (Fig. 3B). First, *CHA1* was disrupted in a ρ^+ *MMF1* background. Second, *MMF1* was disrupted in the *cha1* Δ strain whereas *llv1p* was inhibited by isoleucine in

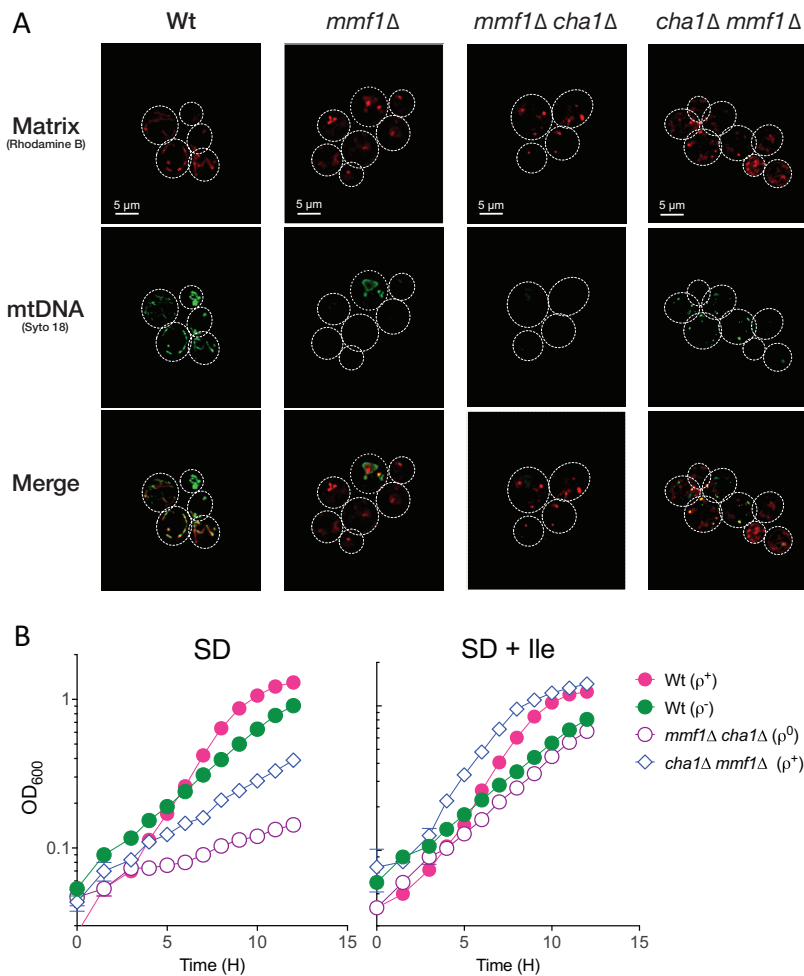


FIG 4 Mmf1p is dispensable for mtDNA maintenance in the absence of 2AA generators. (A) Microscopy ($\times 100$ magnification) confirms that the disruption of *MMF1* prior to *CHA1* led to loss of mtDNA following selection on YPD medium. Conversely, disruption of *CHA1* coupled with feedback inhibition of Ilv1p during propagation on YPD medium preserved mtDNA following the subsequent disruption of *MMF1*. (B) Although the ρ^+ *cha1*Δ *mmf1*Δ mutant maintains respiratory capacity, it remains sensitive to moderate 2AA stress when Ilv1p activity is restored by removing isoleucine from the growth medium. Data displayed are averages and standard deviations of results from three independent cultures.

the YPD-based selection medium. This resulted in a ρ^+ *cha1*Δ *mmf1*Δ double mutant with unique properties. Significantly, introducing the genetic lesions in this order preempted the production of 2AA and resulted in a strain that respired glycerol (Fig. 3B) and maintained its mtDNA (Fig. 4A). Therefore, preventing both Ilv1p and Cha1p serine dehydratase activity renders Mmf1p nonessential for mtDNA maintenance. The inversely constructed *mmf1*Δ *CHA1* strain lost the ability to respire glycerol, and subsequent disruption of *CHA1* in the absence of *MMF1* did not restore growth on glycerol (Fig. 3B). These results demonstrate that disruption of *MMF1* prior to *CHA1* leads to permanent loss of mtDNA, a conclusion supported by mitochondrial staining of the ρ^0 *mmf1*Δ *cha1*Δ strain (Fig. 4A). Thus, identical genotypes constructed in opposing series result in dramatically different outcomes with regard to mtDNA stability. These data support the conclusion that the preemptive disruption of *CHA1*, coupled with isoleucine-mediated inhibition of Ilv1p, blocks 2AA production in the mitochondrial matrix and bypasses the need for Mmf1p to maintain the mitochondrial genome.

The ρ^+ *cha1*Δ *mmf1*Δ mutant maintained wild-type growth indefinitely when propagated on medium containing isoleucine. However, when the inhibition of Ilv1p

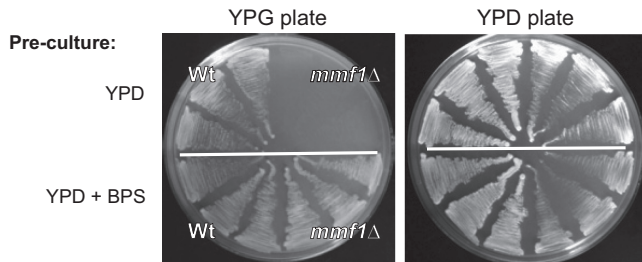


FIG 5 Chelation of iron in the preculture medium preserves the respiratory capacity of *mmf1Δ* mutants. A ρ^+ *mmf1Δ* mutant strain was generated and propagated on YPG medium. Individual colonies from each preculture plate were streaked to YPD or YPD medium containing 10 μ M BPS. After 48 h, three colonies were restreaked (alongside similarly precultured ρ^+ wild-type cultures) on YPG or YPD medium to assess the impact of BPS on maintenance of respiratory capacity during growth on rich dextrose medium.

was lifted by removing isoleucine, a growth defect of the ρ^+ *cha1Δ mmf1Δ* mutant strain ($\mu = 0.18 \pm 0.03$) relative to the ρ^+ wild-type control ($\mu = 0.45 \pm 0.01$) was detected (Fig. 4B). Isoleucine supplementation restored the growth rate (μ) of the ρ^+ *cha1Δ mmf1Δ* strain ($\mu = 0.39 \pm 0.04$) to a level similar to that of the ρ^+ wild-type control ($\mu = 0.48 \pm 0.04$). A parallel result was observed with the respiration-deficient ρ^0 *mmf1Δ cha1Δ* mutant strain where the addition of isoleucine increased the growth rate to the level of the ρ^- wild-type control ($\mu = 0.26$) (Fig. 4B). These data show that the ρ^+ *cha1Δ mmf1Δ* mutant is susceptible to 2AA stress and experiences diminished growth when cultured on minimal medium. However, the respiratory capacity of the ρ^+ *cha1Δ mmf1Δ* mutant was maintained indefinitely during growth on minimal medium (see Fig. S1 in the supplemental material). This result suggests that mtDNA is stable in spite of the growth defect given the moderate level of 2AA stress generated by *Ilv1p* on minimal medium. Enhancing flux through *Ilv1p* to increase 2AA stress severely diminished the ability of the ρ^+ *cha1Δ mmf1Δ* mutant to respire glycerol after growth on minimal medium supplemented with 5 mM serine (Fig. S1). Taken together, these data indicate that in the absence of *Mmf1p*, *Ilv1p* acts on endogenous serine to generate moderate 2AA stress that elicits a minor and reversible growth defect akin to the bacterial paradigm (5). However, exogenous serine stimulates production (via *Ilv1p* and/or *Cha1p*) of sufficient 2AA to cause irreversible loss of the mitochondrial genome.

Availability of iron influences mtDNA stability in the absence of *Mmf1p*. Given the precedents seen in bacterial systems, we theorized that the phenotypes observed for *mmf1Δ* mutants are caused by 2AA inactivation of PLP-dependent enzymes in the yeast mitochondrion. Several PLP-dependent enzymes in the yeast mitochondrion influence iron homeostasis (39, 40), and the disruption of iron homeostasis can lead to mitochondrial iron accumulation, enhanced oxidative stress, and diminished mtDNA stability (41, 42). Therefore, the impact of iron on 2AA-dependent loss of mtDNA was assessed. A ρ^+ *mmf1Δ* (DMY41) mutant was made on yeast extract-peptone-glycerol (YPG) medium as described previously (29). Subsequent transfer of the ρ^+ *mmf1Δ* mutant to YPD medium resulted in the loss of respiratory capacity (Fig. 5). However, transfer of the ρ^+ *mmf1Δ* mutant to YPD medium containing the iron chelator bathophenanthrolinedisulfonic acid (BPS) preserved respiratory capacity (Fig. 5). These data indicate that the loss of mtDNA caused by 2AA stress is contingent on the presence of iron in the growth medium. Sequestration of iron in the growth medium using BPS prevented 2AA-dependent loss of mtDNA, perhaps reflecting that 2AA stress induces accumulation of iron in the mitochondria, leading to damage and eventual loss of mtDNA. These data offer a starting point for future characterization of targets modified by 2AA in the yeast mitochondrion.

DISCUSSION

Our work shows that accumulation of 2AA causes metabolic stress and loss of mtDNA in *S. cerevisiae*. Furthermore, *Mmf1p* prevents 2AA accumulation in the *S. cerevi-*

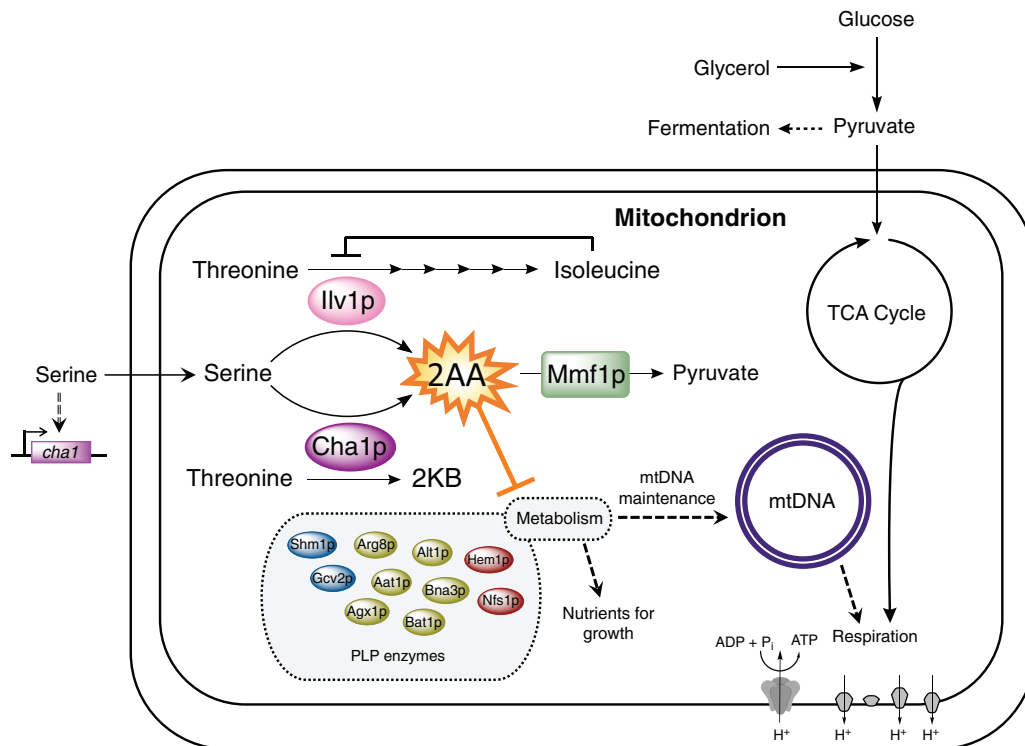


FIG 6 Model of 2AA stress in the yeast mitochondrion. PLP-dependent serine dehydratases active in the yeast mitochondrion (Ilv1p and Cha1p) generate 2AA through the dehydration of serine. Unless Mmf1p is present to prevent 2AA accumulation, metabolic stress arises, ultimately causing loss of the mitochondrial genome. The precedent for 2AA damaging PLP-dependent enzymes suggests that the negative influence of 2AA on mtDNA maintenance is indirect and likely due to damage of one or more target PLP-dependent enzymes. 2KB, 2-ketobutyrate; 2AA, 2-aminoacrylate; CHA1 and ILV1 encode serine/threonine dehydratases (EC 4.3.1.19).

siae mitochondrion. Two consequences of 2AA accumulation in the mitochondrion were identified: the irreversible loss of mtDNA giving rise to respiration-deficient ρ^0 cytoplasmic petites and a transient growth defect on fermentable carbon substrates. The latter phenotype is reminiscent of the growth defects caused by 2AA stress in *S. enterica* (6, 19) and other organisms (8, 28). PLP-dependent enzymes are the only targets of 2AA damage characterized to date (43), suggesting that the *mmf1* Δ strain growth defect is due to inhibition of one or more (of 10 possible) target PLP enzymes in the mitochondrion (44) (Fig. 6). 2AA tested with a bacterial system is not mutagenic *in vivo* (see Table S2 in the supplemental material), making it unlikely that direct DNA damage by 2AA causes the loss of mtDNA. We suggest that loss of mtDNA is caused by the stress that 2AA exerts on the mitochondrial metabolic network. Specifically, we favor a model in which 2AA damages multiple mitochondrial PLP-dependent enzymes, ultimately leading to destabilization and loss of the mitochondrial genome (Fig. 6). The independent disruption of mitochondrial PLP-dependent enzymes involved in heme biosynthesis (Hem1p; EC 2.3.1.37), iron-sulfur cluster biogenesis (Nfs1p; EC 2.8.1.7), one-carbon metabolism (Shm1p; EC 2.1.2.1), and aspartate metabolism (Aat1p; EC 2.6.1.1) has been reported to influence mtDNA stability to various degrees (40, 45–47). Notably, Hem1p and Nfs1p are directly involved in iron metabolism; damage to these enzymes caused by 2AA may underlie the iron sensitivity of *mmf1* Δ mutants. The iron sensitivity of the *mmf1* Δ mutant is reminiscent of that of yeast lacking the frataxin homologue *YFH1* (41, 42), consistent with mitochondrial iron accumulation giving rise to oxidative stress that damages mtDNA. Given the variety of PLP-dependent enzymes that individually impact iron homeostasis and mtDNA stability, it is reasonable to conjecture that the presence of a combination of partially defective enzymes could result in mtDNA loss. Further understanding of how 2AA leads to loss of mtDNA may uncover a novel stress response pathway in mitochondria.

Our work identified a lethal consequence of uncontrolled reactive metabolite accumulation in the mitochondrion. Synthesis of 2AA is unavoidable in PLP-dependent serine dehydration, resulting in the need for RidA proteins (e.g., Mmf1p) to prevent accumulation of this reactive metabolite. Strikingly, when *S. cerevisiae* is exposed to serine, *CHA1* and *MMF1* are the two most highly expressed genes (48), suggesting that these enzymes act in concert to safely reduce serine levels in the mitochondrion. Interestingly, Cha1p is reported to be a component of the mitochondrial nucleoid in *S. cerevisiae* (49), perhaps reflecting an added benefit of Cha1p-dependent physical stabilization of the nucleoid during periods of elevated serine catabolism and 2AA production. The Mmf1p homologue in humans, UK114 (PF01042), is variably described as a tumor antigen, calpain activator, or translation inhibitor in diverse animal cell types (21, 26, 50–52). Importantly, UK114 can substitute for Mmf1p to maintain the mitochondrial genome in *S. cerevisiae* (29), which argues in favor of an evolutionarily conserved biological function. PLP-dependent serine dehydratases are broadly distributed among eukaryotes, which emphasizes the breadth of 2AA stress (53–55). Furthermore, many cell types, including cancer cells and neurons, require high serine levels to promote growth and proliferation (56–58), predisposing certain cell types to high concentrations of a known 2AA precursor. Our work provides a framework for understanding the physiological role of Mmf1p and other eukaryotic RidA proteins, in addition to dissecting the mechanism by which 2AA stress causes loss of mtDNA.

MATERIALS AND METHODS

Strains, media, and chemicals. *Saccharomyces cerevisiae* strain YJF153 (*MATa* HO::*dsdAMX4*) was derived from an oak tree isolate (YPS163) and provided by Justin Fay (Washington University) (32). Rich medium (YP) consisted of 20 g/liter peptone (Fisher Scientific) and 10 g/liter yeast extract (Becton Dickinson). Minimal medium (S medium) contained 1.7 g/liter yeast nitrogen base without amino acids or nitrogen (Sunrise Science; catalog no. 1500-100) and 5 g/liter ammonium sulfate. Either dextrose (D; 20 g/liter) or glycerol (G; 30 g/liter) was provided as the sole carbon source. Solid medium was made by adding 20 g/liter Difco agar (Becton Dickinson). Antibiotics used for deletion marker selection were added at the following final concentrations: 400 μ g/ml Geneticin (G418; Gold Biotechnology), 200 μ g/ml hygromycin B (Gold Biotechnology), and 100 μ g/ml nourseothricin sulfate (cloNAT; Gold Biotechnology). A lower concentration of Geneticin (200 μ g/ml) was used for maintenance of strains with confirmed G418 resistance. Isoleucine or threonine was added to minimal growth medium at a final concentration of 1 mM.

Escherichia coli strain BL21-AI was used for recombinant protein overproduction. Standard *E. coli* growth medium (LB broth) consisted of 10 g/liter tryptone, 5 g/liter yeast extract, and 10 g/liter NaCl. Superbroth containing tryptone (32 g/liter), yeast extract (20 g/liter), sodium chloride (5 g/liter), and sodium hydroxide (0.2 g/liter) was used when high cell densities were required for protein overproduction. Ampicillin (150 μ g/ml) was added to the growth medium as needed. Reagents and chemicals were purchased from Sigma-Aldrich unless otherwise specified.

Genetic techniques and growth methods. Gene disruptions in *S. cerevisiae* were made following the standard gene replacement method described by Hegemann and Heick (59), resulting in the strains listed in Table 1 in the supplemental material. Disruption cassettes were amplified using the appropriate primers and plasmid templates listed in Table S1. Purified DNA (1 μ g) was transformed into *S. cerevisiae* by incubating cells suspended in a mixture of 33% polyethylene glycol 3350 (PEG 3350), 100 mM lithium acetate, and 0.28 mg/ml salmon sperm DNA at 30°C for 30 min followed by 30 min of heat shock at 42°C. The transformed cells were recovered in rich medium containing dextrose (YPD) for 1 h at 30°C and were subsequently plated on solid YPD containing the relevant selection agent. Colonies that arose after 2 to 3 days of incubation were transferred to selective medium, and individual colonies were screened via PCR for the appropriate genetic recombinants. (Additional details of the methods used in the study are provided in Text 1 in the supplemental material.)

For growth analyses, yeast strains were revived from -80°C freezer stocks and streaked for isolation on YPD. Single colonies were inoculated into 2-ml YPD cultures and incubated at 30°C with shaking (200 rpm) overnight. Turbid cultures were (i) 10-fold serially diluted with NaCl for spot plating (10 μ l) on solid medium or (ii) inoculated (1%) into 5 ml of SD medium to monitor growth over time on the basis of the change in optical density at 600 nm (OD_{600}). Growth curves were plotted as averages and standard deviations of results from three independent cultures using GraphPad Prism 7.0. Specific growth rates (μ) were calculated on the basis of the equation $\ln(X/X_0)/T$, where X represents OD_{600} , X_0 is the initial OD_{600} of the linear growth period monitored, and T is time in hours.

Molecular techniques. Plasmids were constructed using standard molecular techniques. DNA was amplified using Q5 DNA polymerase (New England Biolabs) with primers purchased from Eton Bioscience Inc. (Research Triangle Park, NC). Plasmids were isolated using a Wizard Plus SV miniprep kit (Promega), and PCR products were purified using an E.Z.N.A. DNA isolation kit (Omega BioTek). Restriction endonucleases used for molecular cloning were purchased from New England Biolabs. T4 ligase (Thermo Scientific) was used to ligate inserts to vectors. The plasmids and primers used are listed in Table S1.

TABLE 1 Strain list

| Strain | Relevant genotype |
|---------------------|---|
| YJF153 ^a | <i>MATa</i> HO:: <i>dsdAMX4</i> |
| DMy13 | <i>mmf1::kanMX</i> (ρ^0) |
| DMy16 | <i>cha1::hphMX</i> |
| DMy17 | <i>mmf1::kanMX cha1::hphMX</i> (ρ^0) |
| DMy18 | <i>ilv1::natMX</i> |
| DMy20 | <i>cha1::hphMX mmf1::kanMX</i> |
| DMy23 | YJF153 (ρ^-) |
| DMy21 | <i>mmf1::hphMX-loxP</i> (ρ^0) |
| DMy22 | <i>mmf1Δ0</i> (ρ^0) |
| DMy31 | YJF153/pDM1481 |
| DMy32 | YJF153/pSF-empty |
| DMy33 | <i>mmf1Δ0</i> (ρ^0)/pDM1481 |
| DMy34 | <i>mmf1Δ0</i> (ρ^0)/pSF-empty |
| DMy35 | YJF153 (ρ^-)/pDM1481 |
| DMy36 | YJF153 (ρ^-)/pSF-empty |
| DMy41 | <i>mmf1::loxP-kanMX-loxP</i> (ρ^+) |
| DMy43 | <i>ilv1Δ0::ILV1-1^b</i> |
| DMy46 | <i>ilv1Δ0::ILV1-1 mmf1::kanMX</i> |
| DM15531 | <i>E. coli</i> BL21-AI/pDM1463 |
| DM15533 | <i>E. coli</i> BL21-AI/pDM1467 |
| DM15910 | <i>E. coli</i> BL21-AI/pDM1536 |

^aAll yeast strains were constructed in a YJF153 strain background.

^bAllele *ILV1-1* encodes an *Ilv1p*^{R416F} feedback-resistant variant.

Plasmids pUG6, pUG74, and pUG75 were used as templates for drug cassette amplification (EUROSCARF). Plasmid pFA6a-*kanMX* was provided by David Garfinkel (University of Georgia). pSF episomal shuttle vector (Sigma-Aldrich; catalog no. OGS542) containing a *TEF1* promoter, *TPI1* terminator, and Geneticin (yeast)/ampicillin (bacteria) resistance markers was used to express *MMF1* in *S. cerevisiae* (pDM1481); full-length *MMF1* was PCR amplified for cloning using *mmf1_pSF_NcoI_F* and *mmf1_pSF_XbaI_R*. Constructs for protein overproduction were made using pET20b (Novagen) as the vector backbone. Primers were designed to amplify *MMF1* (*mmf1_NdeI_F_truncated_pET20*, *mmf1_XhoI_R*) and *ILV1* (*ilv1_NdeI_F_truncated_pET20*, *ilv1_NotI_R_pET20*) lacking the N-terminal mitochondrial targeting sequences and ligated into pET20b following restriction enzyme digestion of the insertion and vector, forming pDM1463 and pDM1467, respectively. The full-length allele of *ILV1* was cloned into pET20b to make pDM1469. All constructs were transformed into DH5 α following ligation and selected on LB medium containing the appropriate drug. Plasmid insertions were confirmed by sequence analysis performed at Eton Bioscience Inc. Constructs pDM1467 and pDM1469 were used as templates for site-directed mutagenesis to generate pDM1536 and pDM1540, respectively. Site-directed mutants of *ILV1* were made by amplifying pDM1467 and pDM1469 with Q5 polymerase and primer *ilv1_R416F*, changing the codon for arginine-416 (AGA) to phenylalanine-416 (TTC), generating allele *ILV1-1*. Following transformation into DH5 α , site-directed mutants were confirmed by Sanger sequencing (Eton Bioscience). Plasmid pDM1540 served as a template to amplify the *ILV1-1* allele for integration into the chromosome at the *ilv1::natMX* locus of DMy18. Replacement of the *natMX* drug cassette in DMy18 with the feedback-resistant *ILV1-1* allele restored isoleucine prototrophy to DMy43 and abolished nourseothricin sulfate resistance. Integration of the appropriate allele in DMy43 was confirmed by sequence analysis (Eton Bioscience Inc.).

Purification of Mmf1p_(21–147). *Mmf1p*_(21–147), lacking the N-terminal amino acids required for mitochondrial localization, was purified from an *E. coli* BL21-AI strain containing pDM1463. An overnight culture of DM15531 grown in 10 ml of superbroth containing ampicillin was inoculated into 2 liters of superbroth with ampicillin. Cultures were grown for 3 h at 37°C with aeration (200 rpm) until an OD₆₅₀ of 0.5 was reached. Fresh arabinose was added to reach a final concentration of 0.02%, and cultures were shifted to 30°C and incubated for an additional 16 h while being shaken. Cells were harvested by centrifugation and resuspended in binding buffer consisting of 50 mM Tris-HCl (pH 8), 200 mM sodium chloride, 10 mM imidazole, 1 mM TCEP [Tris(2-carboxyethyl)phosphine], and 10% glycerol. Lysozyme (1 mg/ml), phenylmethylsulfonyl fluoride (100 g/ml), and DNase (25 g/ml) were added to the cell suspension, and the reaction mixture was incubated on ice for 1 h. Cells were lysed using a Constant Systems Limited One Shot (United Kingdom) system by passing cells through the disrupter one time with the pressure set to 21,000 lb/in². Following lysis, the extract was clarified, filtered, and injected into a HisTrap high-performance (HP) Ni-Sepharose column (5 ml). The column was washed with five column volumes of binding buffer with 40 mM imidazole added. *Mmf1p* was eluted by increasing the concentration of imidazole from 40 to 300 mM over 10 column volumes, and 3-ml fractions were collected and analyzed by SDS-PAGE to determine protein purity. Fractions containing pure (>99%) protein were pooled and concentrated by centrifugation with a 4,000-molecular-weight-cutoff filter unit (Millipore). The concentrated protein sample was transferred to storage buffer containing 10 mM HEPES and 10% glycerol using a PD-10 desalting column (GE Healthcare). Protein yield as determined using the bicinchoninic acid (BCA) assay (Pierce) was approximately 14 mg/ml. Protein aliquots were frozen in liquid nitrogen and stored at –80°C.

Purification of Ilv1p₍₄₆₋₅₇₆₎ and Ilv1p₍₄₆₋₅₇₆₎R416F. Plasmids encoding His-tagged versions of Ilv1p₍₄₆₋₅₇₆₎ (pDM1467) and Ilv1p₍₄₆₋₅₇₆₎R416F (pDM1536) were transformed into *E. coli* BL21-A1 for protein purification. The resulting strains were inoculated into 10 ml of superbroth containing ampicillin and grown overnight at 37°C. Overnight cultures were subcultured into 2 liters of superbroth containing ampicillin and grown at 37°C until an OD₆₅₀ of 0.7 was reached. Arabinose (0.02%) was added to induce expression, and cultures were shifted to 30°C for 16 h. Cells were harvested at 4°C by centrifugation (15 min at 8,000 × *g*) and resuspended in binding buffer containing 50 mM potassium phosphate (pH 8), 500 mM sodium chloride, 10 mM imidazole, 1 mM TCEP, 10 μM PLP, and 10% glycerol. Lysozyme (1 mg/ml), phenylmethylsulfonyl fluoride (100 g/ml), and DNase (25 g/ml) were added to each cell suspension, which then sat on ice for 1 h. Cells were mechanically lysed using a French pressure cell (5 passes at 10,342 kPa). Each resulting lysate was clarified by centrifugation (45 min at 48,000 × *g*) and filtered through a membrane with 0.45-μm pores. Filtered lysates were loaded onto HisTrap HP Ni-Sepharose columns (5 ml), and the columns were washed with five column volumes of binding buffer containing 40 mM imidazole. Protein was eluted by increasing the concentration of imidazole in the elution buffer from 40 to 300 mM over 10 column volumes. Purified protein was concentrated by centrifugation with a 10,000-molecular-weight-cutoff filter unit (Millipore), and the buffer was replaced with 50 mM Tris-HCl (pH 7.5) containing 10 μM PLP and 10% glycerol using a PD-10 desalting column (GE Healthcare). Protein recovery as determined by the BCA assay (Pierce) was approximately 10.8 mg/ml for Ilv1p₍₄₆₋₅₇₆₎ and 13 mg/ml for Ilv1p₍₄₆₋₅₇₆₎R416F. Protein aliquots were frozen in liquid nitrogen and stored at -80°C.

Ilv1p generation of pyruvate assays. Ilv1p₍₄₆₋₅₇₆₎ serine dehydratase activity was assayed in the presence or absence of Mmf1p or RidA from *S. enterica* as previously described (7). The activity of purified RidA was previously confirmed (3). Reaction mixtures (300 μl) consisted of 50 mM *N*-cyclohexyl-2-aminoethanesulfonic acid (CHES) (pH 9.5), 0.6 μM Ilv1p₍₄₆₋₅₇₆₎, and Mmf1p₍₂₁₋₁₄₇₎ (1.3 μM) or RidA (1.3 μM). Experiments were performed in triplicate, and the results were measured using a 96-well quartz plate and a SpectraMax M2 (Molecular Devices) microplate reader. Reactions were initiated by adding *L*-serine and monitored continuously at 230 nm for 120 s. Initial rates were determined on the basis of the increase in A₂₃₀ corresponding to pyruvate production. A standard curve of pyruvate concentrations relative to A₂₃₀ was generated and used to calculate reaction rates, reported as micromoles of pyruvate produced per minute. The data, reported as averages and standard deviations of results from three independent experiments, were fitted with curves on the basis of the Michaelis-Menten equation using GraphPad Prism 7.0. The procedure described above was used to compare the levels of Ilv1p₍₄₆₋₅₇₆₎ and Ilv1p₍₄₆₋₅₇₆₎R416F catalytic efficiency, with the sole change being that 50 mM potassium phosphate (pH 8) was used instead of 50 mM CHES (pH 9.5).

Inhibition of Ilv1p variants by isoleucine assays. The sensitivity of Ilv1p₍₄₆₋₅₇₆₎ and Ilv1p₍₄₆₋₅₇₆₎R416F to allosteric regulation by isoleucine was determined *in vitro*. Reaction mixtures (300 μl) consisted of 50 mM potassium phosphate (pH 8) and 0.6 μM Ilv1p₍₄₆₋₅₇₆₎ or 0.6 μM Ilv1p₍₄₆₋₅₇₆₎R416F. Isoleucine was added to assays at a final concentration of 3.3 mM. Experiments were performed in triplicate, and the results were measured using a 96-well quartz plate and a SpectraMax M2 (Molecular Devices) microplate reader. Reactions were initiated by adding 120 mM *L*-serine and monitored continuously at 230 nm for 120 s. Initial rates were determined on the basis of the increase in A₂₃₀ corresponding to pyruvate formation. A standard curve of pyruvate concentrations relative to A₂₃₀ was generated and used to calculate reaction rates, reported as micromoles of pyruvate produced per minute. The reaction rates for a single concentration of serine added are reported as averages and standard deviations of results from three independent experiments.

Microscopy. Strains were grown in YPD to full density overnight and then diluted to an OD₆₀₀ of 0.1 in complete synthetic dextrose medium (Sunrise Science; catalog no. 1001-010) the following morning. Cultures were then grown at 30°C and 200 rpm for 4 h. Cells were harvested by centrifugation (2 min at 2,000 × *g*) and resuspended in mounting medium consisting of 10 mM HEPES (pH 7.4) and 5% dextrose. Cells were again pelleted and washed in an equal volume of mounting medium. The mitochondrial matrix was stained with 1 μM rhodamine B (Molecular Probes) for 20 min, followed by 3 min of staining with 10 μM SYTO 18 (Molecular Probes) to detect mitochondrial DNA. Cells were pelleted and resuspended in fresh mounting medium, to which 2 μl of ProLong Live Antifade reagent (Thermo Fisher) was added. Tubes containing cells and antifade reagent were transferred to a sealed box at 4°C overnight. The next morning, 20 μl of cell suspension was mounted on a glass slide and imaged using a DeltaVision microscope system (GE Life Sciences) equipped with an Olympus IX-71 inverted microscope and a xenon arc lamp as the illumination source for exciting the fluorophores. Rhodamine B was visualized with excitation at 555 nm and emission at 627 nm, and SYTO 18 was visualized with excitation at 490 nm and emission at 507 nm. Figures were generated by merging Z stacks of rhodamine B and SYTO 18 images, and the resulting merged images were deconvoluted using a conservative ratio and 15 processing cycles and automated softWoRx 6.5.2 (GE) image acquisition software. A quick projection was generated, and the resulting images were exported to Adobe Illustrator 21.0.2. Images were cropped and resized without adjusting features related to contrast or brightness. Cell borders were generated in Adobe Illustrator by outlining each cell boundary as determined from a white light snapshot.

Impact of iron on respiratory capacity. The *MMF1* locus was disrupted by transforming a ρ⁺ wild-type strain with a drug resistance cassette (*loxP-kanMX-loxP*), and recombinants were selected on YPG medium containing 280 μg/ml Geneticin. Subsequent propagation of the ρ⁺ *mmf1Δ* (DMY41) mutant was done on YPG medium to preserve the mitochondrial genome. The ρ⁺ *mmf1Δ* mutant and a wild-type control were revived from freezer stocks on solid YPG medium and grown overnight at 30°C. Single colonies were picked and streaked onto solid YPD medium or solid YPD medium containing

10 μ M bathophenanthroline disulfonic acid (BPS). Cultures were incubated at 30°C for 48 h, and then three representative colonies were picked from each preculture and restreaked to YPG and YPD plates to assess respiratory capacity. Plates were incubated 48 h at 30°C, and respiration proficiency was assessed on the basis of the ability of strains to grow on glycerol (YPG)-containing medium.

SUPPLEMENTAL MATERIAL

Supplemental material for this article may be found at <https://doi.org/10.1128/mBio.00084-18>.

TEXT S1, DOCX file, 0.1 MB.

FIG S1, EPS file, 12.9 MB.

TABLE S1, DOCX file, 0.3 MB.

TABLE S2, DOCX file, 0.03 MB.

ACKNOWLEDGMENTS

We thank David Garfinkel for technical guidance and David Garfinkel, Zachary Lewis, and Jorge Escalante for critical reading of the manuscript. We thank Justin Fay (Washington University) for generously providing strain YJF153. Muthugapatti Kandasamy (University of Georgia) assisted with microscopy.

This work was supported by funding from the NIH (GM095837) to D.M.D.

REFERENCES

- Lambrecht JA, Schmitz GE, Downs DM. 2013. *RidA* proteins prevent metabolic damage inflicted by PLP-dependent dehydratases in all domains of life. *mBio* 4:e00033-13. <https://doi.org/10.1128/mBio.00033-13>.
- Niehaus TD, Gerdes S, Hodge-Hanson K, Zhukov A, Cooper AJ, ElBadawi-Sidhu M, Fiehn O, Downs DM, Hanson AD. 2015. Genomic and experimental evidence for multiple metabolic functions in the *RidA*/YjgF/YER057c/UK114 (*Rid*) protein family. *BMC Genomics* 16:382. <https://doi.org/10.1186/s12864-015-1584-3>.
- Ernst DC, Lambrecht JA, Schomer RA, Downs DM. 2014. Endogenous synthesis of 2-aminoacrylate contributes to cysteine sensitivity in *Salmonella enterica*. *J Bacteriol* 196:3335–3342. <https://doi.org/10.1128/JB.01960-14>.
- Ernst DC, Anderson ME, Downs DM. 2016. L-2,3-Diaminopropionate generates diverse metabolic stresses in *Salmonella enterica*. *Mol Microbiol* 101:210–223. <https://doi.org/10.1111/mmi.13384>.
- Enos-Berlage JL, Langendorf MJ, Downs DM. 1998. Complex metabolic phenotypes caused by a mutation in *yjgF*, encoding a member of the highly conserved YER057c/YjgF family of proteins. *J Bacteriol* 180:6519–6528.
- Christopherson MR, Schmitz GE, Downs DM. 2008. YjgF is required for isoleucine biosynthesis when *Salmonella enterica* is grown on pyruvate medium. *J Bacteriol* 190:3057–3062. <https://doi.org/10.1128/JB.01700-07>.
- Lambrecht JA, Flynn JM, Downs DM. 2012. Conserved YjgF protein family deaminates reactive enamine/imine intermediates of pyridoxal 5'-phosphate (PLP)-dependent enzyme reactions. *J Biol Chem* 287:3454–3461. <https://doi.org/10.1074/jbc.M111.304477>.
- Borchert AJ, Downs DM. 2017. The response to 2-aminoacrylate differs in *Escherichia coli* and *Salmonella enterica*, despite shared metabolic components. *J Bacteriol* 199:e00140-17. <https://doi.org/10.1128/JB.00140-17>.
- Walsh C. 1982. Suicide substrates: mechanism-based enzyme inactivators. *Tetrahedron* 38:871–909. [https://doi.org/10.1016/0040-4020\(82\)85068-0](https://doi.org/10.1016/0040-4020(82)85068-0).
- Rando RR. 1974. Irreversible inhibition of aspartate aminotransferase by 2-amino-3-butenic acid. *Biochemistry* 13:3859–3863. <https://doi.org/10.1021/bi00716a006>.
- Relyea NM, Tate SS, Meister A. 1974. Affinity labeling of the active center of L-aspartate- β -decarboxylase with β -chloro-L-alanine. *J Biol Chem* 249:1519–1524.
- Wang EA, Kallen R, Walsh C. 1981. Mechanism-based inactivation of serine transhydroxymethylases by D-fluoroalanine and related amino acids. *J Biol Chem* 256:6917–6926.
- Ueno H, Likos JJ, Metzler DE. 1982. Chemistry of the inactivation of cytosolic aspartate aminotransferase by serine O-sulfate. *Biochemistry* 21:4387–4393. <https://doi.org/10.1021/bi00261a030>.
- Likos JJ, Ueno H, Feldhaus RW, Metzler DE. 1982. A novel reaction of the coenzyme of glutamate decarboxylase with L-serine O-sulfate. *Biochemistry* 21:4377–4386. <https://doi.org/10.1021/bi00261a029>.
- Kishore GM. 1984. Mechanism-based inactivation of bacterial kynureninase by beta-substituted amino acids. *J Biol Chem* 259:10669–10674.
- Hillebrand GG, Dye JL, Suelter CH. 1979. Formation of an intermediate and its rate of conversion to pyruvate during the tryptophanase-catalyzed degradation of S-o-nitrophenyl-L-cysteine. *Biochemistry* 18:1751–1755. <https://doi.org/10.1021/bi00576a018>.
- Flynn JM, Christopherson MR, Downs DM. 2013. Decreased coenzyme A levels in *ridA* mutant strains of *Salmonella enterica* result from inactivated serine hydroxymethyltransferase. *Mol Microbiol* 89:751–759. <https://doi.org/10.1111/mmi.12313>.
- Flynn JM, Downs DM. 2013. In the absence of *RidA*, endogenous 2-aminoacrylate inactivates alanine racemases by modifying the pyridoxal 5'-phosphate cofactor. *J Bacteriol* 195:3603–3609. <https://doi.org/10.1128/JB.00463-13>.
- Schmitz G, Downs DM. 2004. Reduced transaminase B (*IlvE*) activity caused by the lack of *yjgF* is dependent on the status of threonine deaminase (*IlvA*) in *Salmonella enterica* serovar Typhimurium. *J Bacteriol* 186:803–810. <https://doi.org/10.1128/JB.186.3.803-810.2004>.
- Christopherson MR, Lambrecht JA, Downs DM. 2012. Suppressor analyses identify threonine as a modulator of *ridA* mutant phenotypes in *Salmonella enterica*. *PLoS One* 7:e43082. <https://doi.org/10.1371/journal.pone.0043082>.
- Farkas A, Nardai G, Csermely P, Tompa P, Friedrich P. 2004. DUK114, the *Drosophila* orthologue of bovine brain calpain activator protein, is a molecular chaperone. *Biochem J* 383:165–170. <https://doi.org/10.1042/BJ20040668>.
- Oka T, Tsuji H, Noda C, Sakai K, Hong YM, Suzuki I, Muñoz S, Natori Y. 1995. Isolation and characterization of a novel perchloric acid-soluble protein inhibiting cell-free protein synthesis. *J Biol Chem* 270:30060–30067. <https://doi.org/10.1074/jbc.270.50.30060>.
- Deaconescu AM, Roll-Mecak A, Bonanno JB, Gerchman SE, Kycia H, Studier FW, Burley SK. 2002. X-ray structure of *Saccharomyces cerevisiae* homologous mitochondrial matrix factor 1 (*Hmf1*). *Proteins* 48:431–436. <https://doi.org/10.1002/prot.10151>.
- Deriu D, Briand C, Mistiniene E, Naktinis V, Grütter MG. 2003. Structure and oligomeric state of the mammalian tumour-associated antigen UK114. *Acta Crystallogr D Biol Crystallogr* 59:1676–1678. <https://doi.org/10.1107/S0907444903014306>.
- Manjasetty BA, Delbrück H, Pham DT, Mueller U, Fieber-Erdmann M, Scheich C, Sievert V, Büsow K, Niesen FH, Weihofen W, Loll B, Saenger W, Heinemann U, Neisen FH. 2004. Crystal structure of *Homo sapiens* protein hp14. *Proteins* 54:797–800. <https://doi.org/10.1002/prot.10619>.
- Michetti M, Viotti PL, Melloni E, Pontremoli S. 1991. Mechanism of action

- of the calpain activator protein in rat skeletal muscle. *Eur J Biochem* 202:1177–1180. <https://doi.org/10.1111/j.1432-1033.1991.tb16487.x>.
27. Antonenkov VD, Ohlmeier S, Sormunen RT, Hiltunen JK. 2007. UK114, a YjgF/Yer057p/UK114 family protein highly conserved from bacteria to mammals, is localized in rat liver peroxisomes. *Biochem Biophys Res Commun* 357:252–257. <https://doi.org/10.1016/j.bbrc.2007.03.136>.
 28. Niehaus TD, Nguyen TND, Gidda SK, ElBadawi-Sidhu M, Lambrecht JA, McCarty DR, Downs DM, Cooper AJL, Fiehn O, Mullen RT, Hanson AD. 2014. *Arabidopsis* and *Maize* RidA proteins preempt reactive enamine/imine damage to branched-chain amino acid biosynthesis in plastids. *Plant Cell* 26:3010–3022. <https://doi.org/10.1105/tpc.114.126854>.
 29. Oxelmark E, Marchini A, Malanchi I, Magherini F, Jaquet L, Hajibagheri MA, Blight KJ, Jauniaux JC, Tommasino M. 2000. Mmf1p, a novel yeast mitochondrial protein conserved throughout evolution and involved in maintenance of the mitochondrial genome. *Mol Cell Biol* 20:7784–7797. <https://doi.org/10.1128/MCB.20.20.7784-7797.2000>.
 30. Kim JM, Yoshikawa H, Shirahige K. 2001. A member of the YER057c/yjgF/UK114 family links isoleucine biosynthesis and intact mitochondria maintenance in *Saccharomyces cerevisiae*. *Genes Cells* 6:507–517. <https://doi.org/10.1046/j.1365-2443.2001.00443.x>.
 31. Megraw TL, Chae CB. 1993. Functional complementarity between the HMG1-like yeast mitochondrial histone HM and the bacterial histone-like protein HU. *J Biol Chem* 268:12758–12763.
 32. Li XC, Fay JC. 2017. Cis-regulatory divergence in gene expression between two thermally divergent yeast species. *Genome Biol Evol* 9:1120–1129. <https://doi.org/10.1093/gbe/evx072>.
 33. Day M. 2013. Yeast petites and small colony variants: for everything there is a season. *Adv Appl Microbiol* 85:1–41. <https://doi.org/10.1016/B978-0-12-407672-3.00001-0>.
 34. Ryan ED, Kohlhaw GB. 1974. Subcellular localization of isoleucine-valine biosynthetic enzymes in yeast. *J Bacteriol* 120:631–637.
 35. Bornaes C, Ignjatovic MW, Schjerling P, Kielland-Brandt MC, Holmberg S. 1993. A regulatory element in the CHA1 promoter which confers inducibility by serine and threonine on *Saccharomyces cerevisiae* genes. *Mol Cell Biol* 13:7604–7611. <https://doi.org/10.1128/MCB.13.12.7604>.
 36. Ahmed SI, Bollon AP, Rogers SJ, Magee PT. 1976. Purification and properties of threonine deaminase from *Saccharomyces cerevisiae*. *Biochimie* 58:225–232. [https://doi.org/10.1016/S0300-9084\(76\)80374-4](https://doi.org/10.1016/S0300-9084(76)80374-4).
 37. Chen L, Chen Z, Zheng P, Sun J, Zeng AP. 2013. Study and reengineering of the binding sites and allosteric regulation of biosynthetic threonine deaminase by isoleucine and valine in *Escherichia coli*. *Appl Microbiol Biotechnol* 97:2939–2949. <https://doi.org/10.1007/s00253-012-4176-z>.
 38. Ernst DC, Downs DM. 2015. 2-aminoacrylate stress induces a context-dependent glycine requirement in *ridA* strains of *Salmonella enterica*. *J Bacteriol* 198:536–543. <https://doi.org/10.1128/JB.00804-15>.
 39. Song JY, Marszalek J, Craig EA. 2012. Cysteine desulfurase Nfs1 and Pim1 protease control levels of Isu, the Fe-S cluster biogenesis scaffold. *Proc Natl Acad Sci U S A* 109:10370–10375. <https://doi.org/10.1073/pnas.1206945109>.
 40. Sliwa D, Dairou J, Camadro JM, Santos R. 2012. Inactivation of mitochondrial aspartate aminotransferase contributes to the respiratory deficit of yeast frataxin-deficient cells. *Biochem J* 441:945–953. <https://doi.org/10.1042/BJ20111574>.
 41. Radisky DC, Babcock MC, Kaplan J. 1999. The yeast frataxin homologue mediates mitochondrial iron efflux. Evidence for a mitochondrial iron cycle. *J Biol Chem* 274:4497–4499. <https://doi.org/10.1074/jbc.274.8.4497>.
 42. Gakh O, Park S, Liu G, Macomber L, Imlay JA, Ferreira GC, Isaya G. 2006. Mitochondrial iron detoxification is a primary function of frataxin that limits oxidative damage and preserves cell longevity. *Hum Mol Genet* 15:467–479. <https://doi.org/10.1093/hmg/ddi461>.
 43. Downs DM, Ernst DC. 2015. From microbiology to cancer biology: the Rid protein family prevents cellular damage caused by endogenously generated reactive nitrogen species. *Mol Microbiol* 96:211–219. <https://doi.org/10.1111/mmi.12945>.
 44. Whittaker JW. 2016. Intracellular trafficking of the pyridoxal cofactor. Implications for health and metabolic disease. *Arch Biochem Biophys* 592:20–26. <https://doi.org/10.1016/j.abb.2015.11.031>.
 45. Whittaker MM, Penmatsa A, Whittaker JW. 2015. The Mtm1p carrier and pyridoxal 5'-phosphate cofactor trafficking in yeast mitochondria. *Arch Biochem Biophys* 568:64–70. <https://doi.org/10.1016/j.abb.2015.01.021>.
 46. Luzzati M. 1975. Isolation and properties of a thymidylate-less mutant in *Saccharomyces cerevisiae*. *Eur J Biochem* 56:533–538. <https://doi.org/10.1111/j.1432-1033.1975.tb02259.x>.
 47. Li J, Kogan M, Knight SA, Pain D, Dancis A. 1999. Yeast mitochondrial protein, Nfs1p, coordinately regulates iron-sulfur cluster proteins, cellular iron uptake, and iron distribution. *J Biol Chem* 274:33025–33034. <https://doi.org/10.1074/jbc.274.46.33025>.
 48. Godard P, Urrestarazu A, Vissers S, Kontos K, Bontempi G, van Helden J, André B. 2007. Effect of 21 different nitrogen sources on global gene expression in the yeast *Saccharomyces cerevisiae*. *Mol Cell Biol* 27:3065–3086. <https://doi.org/10.1128/MCB.01084-06>.
 49. Chen XJ, Wang X, Kaufman BA, Butow RA. 2005. Aconitase couples metabolic regulation to mitochondrial DNA maintenance. *Science* 307:714–717. <https://doi.org/10.1126/science.1106391>.
 50. Bussolati G, Geuna M, Bussolati B, Millesimo M, Botta M, Bartorelli A. 1997. Cytolytic and tumor inhibitory antibodies against UK114 protein in the serums of cancer patients. *Int J Oncol* 10:779–785. <https://doi.org/10.3892/ijo.10.4.779>.
 51. Funaro A, Horenstein AL, Ghisolfi G, Bussolati B, Bartorelli A, Bussolati G. 1999. Identification of a 220-kDa membrane tumor-associated antigen by human anti-UK114 monoclonal antibodies selected from the immunoglobulin repertoire of a cancer patient. *Exp Cell Res* 247:441–450. <https://doi.org/10.1006/excr.1998.4384>.
 52. Rorbach J, Minczuk M. 2012. The post-transcriptional life of mammalian mitochondrial RNA. *Biochem J* 444:357–373. <https://doi.org/10.1042/BJ20112208>.
 53. Snell K. 1984. Enzymes of serine metabolism in normal, developing and neoplastic rat tissues. *Adv Enzyme Regul* 22:325–400. [https://doi.org/10.1016/0065-2571\(84\)90021-9](https://doi.org/10.1016/0065-2571(84)90021-9).
 54. Sun L, Bartlam M, Liu Y, Pang H, Rao Z. 2005. Crystal structure of the pyridoxal-5'-phosphate-dependent serine dehydratase from human liver. *Protein Sci* 14:791–798. <https://doi.org/10.1110/ps.041179105>.
 55. Yamada T, Komoto J, Kasuya T, Takata Y, Ogawa H, Mori H, Takusagawa F. 2008. A catalytic mechanism that explains a low catalytic activity of serine dehydratase like-1 from human cancer cells: crystal structure and site-directed mutagenesis studies. *Biochim Biophys Acta* 1780:809–818. <https://doi.org/10.1016/j.bbagen.2008.01.020>.
 56. Labuschagne CF, van den Broek NJF, Mackay GM, Voudsen KH, Maddocks ODK. 2014. Serine, but not glycine, supports one-carbon metabolism and proliferation of cancer cells. *Cell Rep* 7:1248–1258. <https://doi.org/10.1016/j.celrep.2014.04.045>.
 57. Amelio I, Cutruzzolà F, Antonov A, Agostini M, Melino G. 2014. Serine and glycine metabolism in cancer. *Trends Biochem Sci* 39:191–198. <https://doi.org/10.1016/j.tibs.2014.02.004>.
 58. de Koning TJ, Snell K, Duran M, Berger R, Poll-The BT, Surtees R. 2003. L-Serine in disease and development. *Biochem J* 371:653–661. <https://doi.org/10.1042/BJ20021785>.
 59. Hegemann JH, Heick SB. 2011. Delete and repeat: a comprehensive toolkit for sequential gene knockout in the budding yeast *Saccharomyces cerevisiae*. *Methods Mol Biol* 765:189–206. https://doi.org/10.1007/978-1-61779-197-0_12.